

Ginger (*Zingiber officinale*)-Mediated Green Synthesis of Silver-Doped Tin Oxide Nanoparticles and Evaluation of Its Antimicrobial Activity

Yobsan Likasa Tiki, Leta Deressa Tolesa, Ardila Hayu Tiwikrama, and Tolesa Fita Chala*



Cite This: *ACS Omega* 2024, 9, 11443–11452



Read Online

ACCESS |

Metrics & More

Article Recommendations

Supporting Information

ABSTRACT: Green synthesis of nanoparticles using plant extract is a novel development that has gained significant attention because of its low cost, nontoxicity, and environmental friendliness. In the present study, silver-doped stannic oxide (Ag-doped SnO₂) nanoparticle was synthesized by an eco-friendly green synthesis method. The synthesized samples were characterized using scanning electron microscopy (SEM), Fourier transform infrared spectroscopy (FTIR), ultraviolet–visible spectroscopy (UV–vis), X-ray diffraction (XRD), and their antimicrobial activities were assessed against two bacteria *Escherichia coli* (*E. coli*) and *Staphylococcus aureus* (*S. aureus*) and two fungi *Fusarium oxysporum* (*F. oxysporum*) and *Fusarium graminearum* (*F. graminearum*) by using the disk diffusion method. Ag-doped SnO₂ nanoparticles show a strong and broad absorption from UV–vis spectra when compared to pure SnO₂ nanoparticles. FTIR spectral analysis revealed that the peak at 505.69 cm⁻¹ was assigned to Sn–O and O–Sn–O stretching vibration of SnO₂ nanoparticles. XRD analysis confirmed the formation of a tetragonal rutile structure with average particle size ranging from 10 to 17 nm. The antimicrobial result indicates that the Ag-doped SnO₂ revealed significant antimicrobial activity against both bacterial and fungi strains with the zone of inhibition of 29 ± 0.54, 27 ± 0.05, 17 ± 0.05, and 15 ± 0.05 mm for *S. aureus*, *E. coli*, *F. oxysporum*, and *F. graminearum*, respectively. Thus, the studies suggested that Ag-doped SnO₂ nanoparticles exhibit good activity against both Gram-negative and Gram-positive bacteria and fungi. This is because doping SnO₂ nanoparticles with metallic elements such as Ag has been used to enhance their performance, confirming them as a good candidate for antimicrobial agents and the development of future therapeutic agents



1. INTRODUCTION

It is quite concerning that infectious diseases continue to spread and that harmful bacteria and fungi are rapidly developing medication resistance. Morbidity and mortality related to microbial infections are still high despite advances in our understanding of microbial pathophysiology and the application of contemporary treatments.¹ To create the next generation of medications or agents to control microbial diseases, it is urgently necessary to identify new antimicrobial agents from natural and inorganic substances. The toxicity of organic chemicals used for disinfection is one of its disadvantages. As a result, inorganic disinfectants like metal oxide nanoparticles are attracting more attention.² Bacterial strains can be effectively inhibited by metal oxide nanoparticles. Metal oxide nanoparticles' antibacterial activity is influenced by their size, the presence of light, the makeup of the aqueous medium used for the test, and other factors.³

Nanoparticles' (NPs) binding to the bacterium is caused by electrostatic interactions. By altering the integrity of the bacteria's cell membrane and releasing harmful free radicals, these interactions put the bacteria under oxidative stress.^{3,4}

The number of constituent atoms located surrounding the surface of the particles increases as the particle size drops to a certain point, creating highly reactive particles with various physical, optical, chemical, and electrical properties. Therefore, it is vital to manipulate and control material properties.^{5,6} The synthesis of nanoparticles using chemical approaches is toxic and produces nonenvironmentally friendly byproducts. Growing interest in biological methods that do not produce harmful chemicals as byproducts is being driven by the demand for ecologically safe synthesis processes for nanoparticle synthesis.⁷ In order to develop practical, nontoxic, natural products for the generation of metal oxide nanoparticles in aquatic environments, the use of green nanotechnology has attracted attention.^{6,8} A growing trend in green nano-

Received: October 9, 2023
Revised: February 10, 2024
Accepted: February 13, 2024
Published: February 27, 2024



technology is the development of practical, nontoxic, and natural products for the production of metal oxide nanoparticles in aquatic environment.⁹

The use of plants in the green synthesis of metal oxide nanoparticles has drawn increasing attention as a viable substitute for chemical and physical procedures. The green synthesis approach for the synthesis of metal nanoparticles has several advantages over conventional methods among the various methods described in the literature because it is simple, economical, environmentally friendly, and uses bioresources (plants, fungi, algae, and microorganisms) that can act as reducing agents, stabilizers, and capping agents the formation of nanoparticles.^{7,10–14}

Ginger extract contains a variety of active metabolites including volatile and nonvolatile compounds, such as gingerol, paradols, shogaol, alkaloids, flavonoids, and zingerone, which are believed to possess distinctive medicinal and biological properties.¹⁵ The bioactive compounds of ginger extract can serve as reducing and stabilizing agents for the synthesis of nanomaterials.^{16–18} The use of ginger extract promotes a green synthesis approach, aligning with sustainable and environmentally friendly practices. It minimizes the need for harsh chemicals and reduces the environmental impact often associated with conventional synthesis.¹⁹ The bioactive compounds in ginger are known for their biocompatibility and low toxicity, making ginger extract a favorable choice for biomedical applications.²⁰ Therefore, Ginger extract, chosen as the raw material for the synthesis of nanomaterials, offers several distinct advantages owing to its unique chemical composition and functional properties.

Tin(IV) oxide (SnO_2) is an n-type semiconductor with a band gap $E_g = 3.6$ eV. Among the nanometallic oxides, SnO_2 is employed for a variety of potential applications in environmental remediation, gas sensing, catalysts, dye-based solar cells, lithium-ion batteries, light-emitting devices, and optoelectronic materials.^{21–26} This metal oxide is being researched for its potential antibacterial properties in addition to these outstanding applications.^{27–29} Ag modified the mechanical characteristics of nanoparticles and improved their antibacterial activity.³⁰ Silver-doped metal oxide nanomaterials show outstanding antibacterial properties due to the synergistic actions of reactive oxygen species (ROS) and Ag^+ , which can cause protein and DNA denaturation and speed up bacterial death.^{31,32} Ag-doped SnO_2 nanoparticles can also exhibit relatively low cytotoxicity in comparison to other nanomaterials.^{33,34} In addition to antibacterial properties, silver-doped SnO_2 nanoparticles cover a wide range of applications in the field of sensors, photocatalysis, energy storage, solar cells, and coating materials.^{35–39} Doping materials with metal oxide atoms is a successful method for modifying the structural, thermal, and morphological qualities to optimize the distinctive properties, according to earlier studies.⁴⁰ In order to enhance the SnO_2 's distinctive features, several elements such as Ni, Fe, Zn, Au, and Co have been doped.^{27,41–43} To the best of our knowledge, no studies have been reported on the green synthesis of silver-doped SnO_2 nanoparticles using ginger (*Zingiber officinale*) root extraction and assessments of its antimicrobial activity. As a result, the current work concentrates on green synthesis, characterization of Ag-doped SnO_2 nanoparticles using the ginger (*Z. officinale*) root extracted, and evaluation of antimicrobial efficacy against human pathogenic bacteria and fungi.

2. MATERIAL AND METHODS

2.1. Chemicals and Reagents. The chemicals and reagents used in this work are tin chloride ($\text{SnCl}_4 \cdot 5\text{H}_2\text{O}$, 99%), deionized water (DI), nutrient agar granulated (95%), agar-agar type 1 (95%), bacteria pure culture (100%), silver nitrate (AgNO_3), ethanol (CH_3OH , 98%), nutrient broth, nutrient agar, agar-agar, petri dishes, antibiotic discs, cotton swabs. All chemicals were of analytical grade and used without further purification.

2.2. Preparation of the Ginger Root Extract. The fresh, ginger (*Z. officinale*) roots were collected from Nopha district Ilu Abba Boor Zone, Oromia, Ethiopia. The collected and dried ginger roots were pulverized to fine dust by using an electric grinder and preserved in plastic containers. The extracts of ginger root powder were prepared by mixing 10 g with 100 mL of 70% acetone under vigorous stirring for 15 min, kept for 48 h at room temperature, and filtered through Whatman No.1 filter paper. The extract was heated at 70 °C for 20 min to remove acetone and then cooled at room temperature. Then the filtrate was stored in a refrigerator at 4 °C in order to be used for further experiments.^{44,45}

2.3. Green Synthesis of SnO_2 Nanoparticles. The green synthesis of pure SnO_2 NPs was carried out by taking 20 mL of ginger and diluted to 100 mL. Then, it was dropwise added into 60 mL of $\text{SnCl}_4 \cdot 5\text{H}_2\text{O}$ (0.5 M) solution with constant stirring at room temperature for 30 min. The stirring of the solution continued for another 30 min at 80 °C. Then, the obtained solution was cooled and then washed the resulting precipitates several times with double ethanol and dried in an oven at 70 °C for 36 h. The yielded black solid was then crushed using a mortar and pestle. Then, the calcination of the solid was carried out at 350 °C for 2 h.^{43,46}

2.4. Green Synthesis of Ag-Doped SnO_2 Nanoparticles. The $\text{Ag}_{1-x}\text{NO}_3$ ($x = 0.2, 0.4, 0.6, 0.8,$ and 1.0) dopants were prepared by dissolving 1.60, 2.60, 4.40, 5.28, and 6.60 mmol AgNO_3 of solution in the synthesized (6.6 mmol) of SnO_2 nanoparticles in Section 2.3. Then, 60 mL of ginger extract was added wisely to each solution of AgNO_3 ($x = 0.2, 0.4, 0.6, 0.8,$ and 1.0) and (6.6 mmol) SnO_2 nanoparticles under constant stirring at 70 °C for 30 min to complete the white precipitate of Ag-doped SnO_2 composite particles. Then, the obtained precipitate was filtered and washed five times with ethanol, followed by air-drying for 48 h at room temperature, and after grinding, the powder was annealed for 4 h at 400 °C a dark gray colored powder of Ag-doped SnO_2 nanoparticles was prepared. Finally, the sample was named as 0.2Ag-doped SnO_2 , 0.4Ag-doped SnO_2 , 0.6Ag-doped SnO_2 , 0.8Ag-doped SnO_2 , and 1.0Ag-doped SnO_2 nanoparticles.^{47,48}

2.5. Characterization. Absorption spectra of Ag-doped SnO_2 nanoparticles were analyzed using UV–vis absorption spectrophotometer T80⁺ in the range of 200–800 nm. The crystalline structure of the green synthesized nanoparticles was analyzed using a Bruker D2 phaser X-ray diffractometer with graphite monochromatic Cu K-alpha radiation ($\lambda = 1.54056$ Å) in the range of 2θ angles 10° to 80°. Fourier Transform infrared spectrophotometer PerkinElmer LX185255 was used to measure the bond formation of Ag- SnO_2 in the scanning range of 400–4000 cm^{-1} . The morphologies of the samples were characterized via scanning electron microscopy (SEM, SM6500F, JEOL, Tokyo, Japan)

2.6. Evaluation of Antimicrobial Activity. The antimicrobial activity of synthesized pure SnO_2 and Ag-doped

SnO₂ NPs was assessed against bacteria (*S. aureus* and *E. coli*) and fungi (*F. oxysporum* and *F. graminearum*) using the disc diffusion method. For pure SnO₂ and Ag-doped SnO₂ nanoparticles, the concentrations (3, 3.5, 4, 4.5, 5, and 5.5 mg/mL) were prepared separately in distilled water. All the plates were incubated overnight at 37 °C for 24 h. When the incubation period was over the Petri plates were taken out from the incubator and the diameters of zones produced around the wells were examined and recorded. The zone of inhibitions around each well is measured by using a caliper in millimeters (mm). Standard reference antibiotics docmymicine and propiconazole were taken as positive control and distilled water served as a negative control. The effectiveness of test samples for pure SnO₂ and Ag-doped SnO₂, doxycycline, propiconazole, and distilled water on bacterial and fungi strains was assessed by measuring zone inhibition of bacterial growth conditions at 37 °C

3. RESULT AND DISCUSSION

3.1. Qualitative Phytochemical Analysis. Phytochemicals are chemical substances derived from plants and used to describe the large number of secondary metabolic compounds found in plants. The phytochemical screening assay is a simple, rapid, and inexpensive procedure that gives researchers a quick answer to the different types of phytochemicals in a mixture and is an important tool for the analysis of bioactive compounds. The presence of secondary metabolite groups in ginger (*Z. officinale*) was determined by preliminary phytochemical analysis using typical prospection standard methods.⁴⁹ The presence of the bioactive compound in the ginger extract can trigger the reduction of metal salts (AgCl and SnCl₄·5H₂O) and control the size of synthesized Ag-doped SnO₂ NPs. Furthermore, the results of the qualitative phytochemical analysis of the ginger root extract are shown in Figure 1 and (Supporting Information Table S1). The

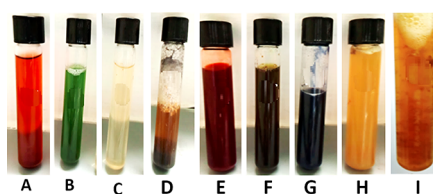


Figure 1. Qualitative phytochemical analysis for the presence of (A) alkaloids, (B) tannins, (C) flavonoids, (D) saponins, (E) terpenoids, (F) phenols, (G) carbohydrates, (H) steroids, and (I) oils and fats in ginger (*Z. officinale*) root extract.

preliminary phytochemical studies revealed that alkaloids, tannins, phenols, flavonoids, terpenoids, and glycosides were present in the plant extract. Thus, the ginger root extracts consist of phytochemicals capable of reducing Ag⁺ and Sn⁴⁺ by donating electrons, covering, and stabilizing the nanoparticles formed.^{10,50}

3.2. Green Synthesis of Ag-Doped SnO₂ Nanoparticles. Ginger (*Z. officinale*) root extract contains biomolecules such as alkaloids, flavonoids, glycosides, terpenoids, tannins, and phenols which aid in the synthesis of Ag-doped SnO₂ nanoparticles. These biomolecules present in the ginger root acted as the reducing, capping, and stabilizing agents for the synthesis of the nanoparticles.^{7,45,51} During the synthesis of Ag-doped SnO₂ Nps the color changed from an orange color to a white precipitate after constant

stirring for 30 min indicating the formation of Ag-doped SnO₂ as shown in Figure 2. Finally, the color of synthesized Ag-

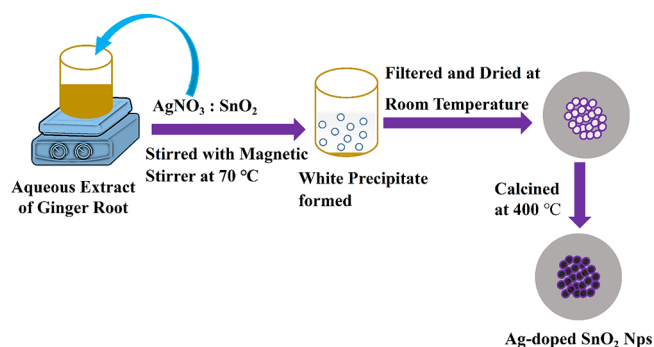


Figure 2. Schematic representation for green synthesis of Ag-doped SnO₂ nanoparticles.

doped SnO₂ changed from white to dark gray after calcination at 400 °C for 4 h. The color change may be due to the plasmonic properties of silver nanoparticles.⁵² Moreover, the schematic representation for the synthesis of Ag-doped SnO₂ nanoparticles is shown in Figure 2.

3.3. Characterizations of the Samples. The UV–vis absorption spectra of pure SnO₂ and Ag-doped SnO₂ nanoparticles are presented in Figure 3A in order to confirm the absorption capability of prepared samples. The obtained result showed that the Ag-doped SnO₂ nanoparticles exhibit broad absorption in the wavelength range of 300–800 nm when compared to pure SnO₂ nanoparticles. Moreover, as the concentration of Ag dopant increases, the absorption spectra wavelength switches to a higher wavelength or causes a redshift. Thus, increasing the silver doping causes a rise in O vacancies and likely creates a new doubly occupied O vacancy. This implies that the band gap shift and absorption of the doped nanoparticles may be influenced by surface effects, doping-induced vacancies, and lattice strain.⁵³

Moreover, the band gap energy (E_g) of the prepared samples was determined by using Tauc's equation⁴⁸ and presented in Figure 3B. The band gap energy (E_g) values were estimated by extrapolation of the linear part of the curves obtained by plotting $(\alpha h\nu)^2$ versus $h\nu$, where α is the absorption coefficient and $h\nu$ is photon energy. Therefore, the calculated band gap energy (E_g) is 3.57, 3.41, 3.29, 3.19, and 3.08 eV for pure SnO₂, 0.2Ag-doped SnO₂, 0.4Ag-doped SnO₂, 0.6Ag-doped SnO₂, 0.8Ag-doped SnO₂ nanoparticles, respectively. The band gap energy decreased to 3.08 eV when Ag is doped into the SnO₂ matrix and this is due to electron transition energy.^{54,55}

FTIR spectra of undoped SnO₂ and Ag-doped SnO₂ nanoparticles were recorded in the range of 4000–400 cm⁻¹ and presented in Figure 4. As can be seen, the peaks observed at 3380.658, 1629.584, 1366.05, 1236.73, 1083.69, and 505.6956 cm⁻¹ are attributed to green synthesized pure SnO₂ Nps. The broad band around 3380.68–1618 cm⁻¹ is due to stretching vibrations of Sn–OH groups and O–H stretching vibrations of water molecules may be absorbed on the surface of nanoparticles. The vibration bands at 505.69 cm⁻¹, particularly, were attributed to the O–Sn–O bending and stretching vibration of Sn–O, which made up the band between 400 and 700 cm⁻¹. These bands indicate the formation of SnO₂ nanoparticles.^{56,57} Similarly, the peak observed between 400 and 622.239 cm⁻¹ is ascribed to the metal–oxygen (M–O) bond of Sn–O stretching vibrations.

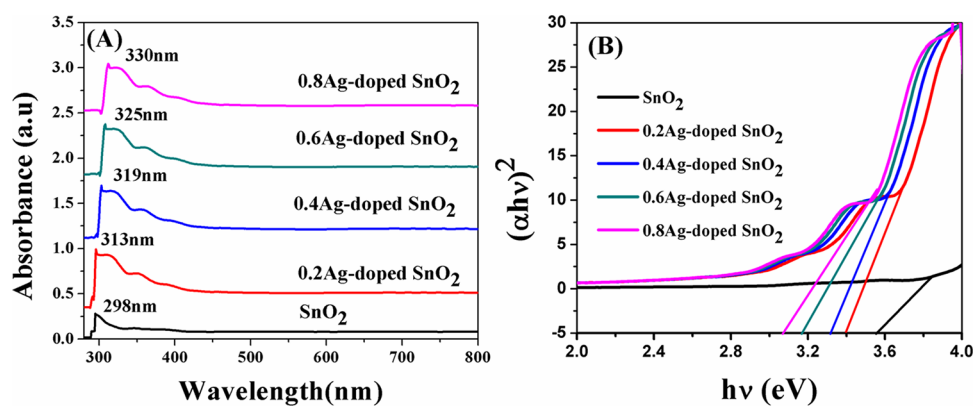


Figure 3. (A) UV-vis spectra of undoped SnO₂ and Ag-doped SnO₂ Nps and (B) plots of the $(\alpha h\nu)^2$ versus photon energy ($h\nu$) for the band gap energy of undoped SnO₂ and Ag-doped SnO₂ NPs with (0.2Ag-doped SnO₂, 0.4Ag-doped SnO₂, 0.6Ag-doped SnO₂, 0.8Ag-doped SnO₂ NPs).

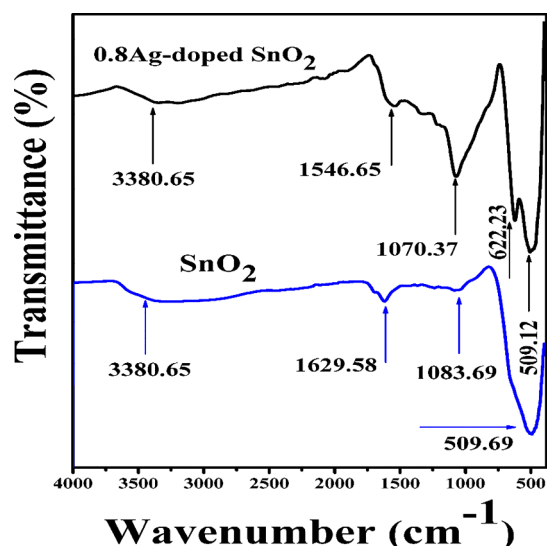


Figure 4. FTIR spectra of green synthesized pure SnO₂ and 0.8Ag-doped SnO₂ NPs.

The absorption peaks observed at 622.239 cm^{-1} are assigned to the Ag–O–Sn bonding of the Ag-doped SnO₂ composite particles.^{48,58}

The crystal structure of green synthesized pure SnO₂ and Ag-doped SnO₂ nanoparticles were investigated by X-ray diffraction pattern and shown in Figure 5. The 2θ values of the prepared samples were scanned in the range of 10° to 80° . As can be seen in Figure 5, the diffraction peaks at 2θ values of 27.03° , 28.27° , 29.50° , 32.68° , 34.31° , 38.49° , 42.01° , 46.70° , 52.15° , 55.27° , 57.95° can be assigned to lattice plane reflections of (111), (110), (200), (002), (210), (211), (220), (221), (300), (311), and (231) respectively for both pure SnO₂ and Ag-doped SnO₂ nanoparticles based on the JCPDS card No. 41-1445.⁴⁸ This confirms that the prepared samples are naturally well crystalline and have a tetragonal structure.³² Therefore, the characteristic peaks that have been obtained for Ag-doped SnO₂ nanoparticles are in good agreement with the previously reported literature.^{59,60} Additionally, as the silver dopant increased (0.2, 0.4, 0.6, and 0.8), the diffraction peak's intensity decreased relative to pure SnO₂. Similarly, there is a slight broadening in XRD peaks at different diffraction peaks of silver doping revealing that the particle size decreased, and this is due to the impacts of disruptions or defects generated by silver ions in the structure of the

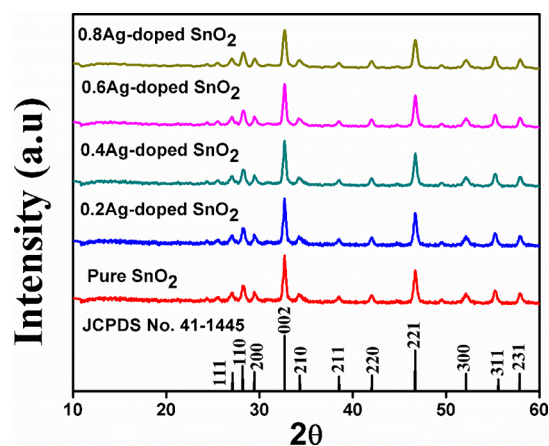


Figure 5. XRD of patterns of green synthesized pure SnO₂, 0.2Ag-doped SnO₂, 0.4Ag-doped SnO₂, 0.6Ag-doped SnO₂, and 0.8Ag-doped SnO₂ nanoparticles.

SnO₂.^{61,62} The crystalline sizes of the as-synthesized samples were calculated using Scherer's equation.⁶³

$$D = \frac{K\lambda}{\beta \cos \theta} \quad (1)$$

where D is the average particle size, K is a dimensionless factor, which is close to unity, λ is the wavelength of X-ray radiation, β is the full width at half-maxima (fwhm) of the diffraction peak of highest intensity, and θ is the Bragg angle of X-ray. Thus, the average crystallite sizes for pure SnO₂, 0.2Ag-doped SnO₂, 0.4Ag-doped SnO₂, 0.6Ag-doped SnO₂, and 0.8Ag-doped SnO₂ were found to be 16.79, 12.88, 11.29, 10.29, and 9.59 nm, respectively.

The morphology of the green synthesized SnO₂ and Ag-doped SnO₂ nanoparticles was investigated by using Scanning Electron Microscopy (SEM) and shown in Figure 6A,B. It is clearly seen that the SEM image of pure SnO₂ and Ag-doped is agglomerated and shows an irregular shape of morphology. The average particle size of the nanoparticles ranged from 15 to 30 nm. The particles exist as the tetragonal structure of SnO₂ nanoparticles^{64,65} which is a good agreement with X-ray diffraction analysis.

The elemental composition of Pure SnO₂ and Ag-doped SnO₂ nanoparticles was examined using energy-dispersive X-ray (EDX), as shown in Figure 6C,D. Accordingly, the EDX spectra of pure SnO₂ nanoparticles showed that they were

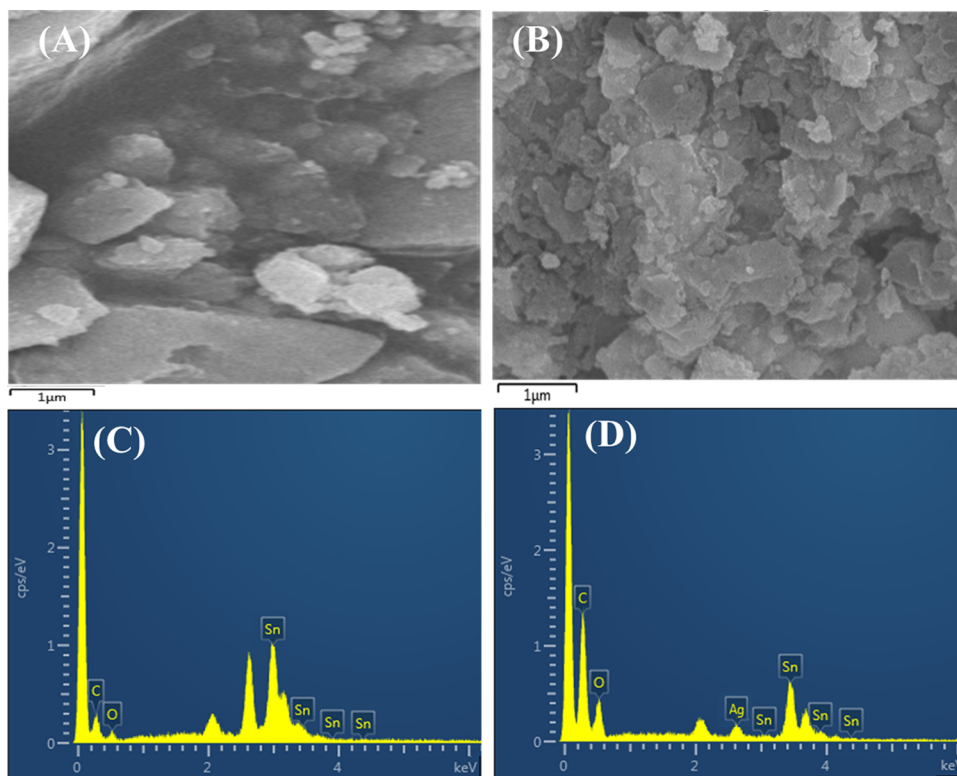


Figure 6. Scanning electron microscopy (SEM) of undoped SnO₂ (A) and Ag-doped SnO₂ Nps (B) and energy-dispersive X-ray (EDX) spectrum of undoped SnO₂ (C) and Ag-doped SnO₂ Nps (D).

entirely composed of Sn and O elements, as shown in Figure 6C. Similarly, the EDS spectra of Ag-doped SnO₂ nanoparticles presented in Figure 6D confirm the presence of Ag, Sn, and O elements, suggesting that Ag has been successfully doped into SnO₂. Therefore, this results in strong evidence that the silver ions have been successfully incorporated into the SnO₂ nanoparticle.^{36,38,48} The presence of signal carbon may come from the sample holder during the characterization of the samples.⁶⁶

In addition, in order to confirm that Ag was successfully incorporated into SnO₂ nanoparticles EDX mapping analysis were performed for Ag-doped SnO₂ nanoparticles. Accordingly, the elemental mapping analysis on the dopant nanoparticles reveals the presence of Ag, Sn, and O in Ag-doped SnO₂ nanoparticles and it is depicted in Figure 7A–D. These all findings provided conclusive proof that Ag nanoparticles were effectively doped into SnO₂ nanoparticles³⁶

3.4. Evaluation of Antimicrobial Activity. The antimicrobial activity of the prepared Ag-doped SnO₂ NPs was examined against two pathogenic bacteria (*S. aureus* and *E. coli*) and two pathogenic fungi (*F. oxysporum* and *F. graminearum*) and shown in Table 1 and (Figure S1 in the Supporting Information). After 24 h of incubation at 37 °C, the growth of the bacterial samples was evaluated against the green-produced Ag-doped SnO₂ nanoparticles. By establishing the zone of inhibition against *S. aureus*, *E. coli*, and fungi, the antibacterial activity of Pure SnO₂, 0.2Ag-doped SnO₂, 0.4Ag-doped SnO₂, 0.6Ag-doped SnO₂, 0.8Ag-doped SnO₂, and 1.0Ag-doped SnO₂ was assessed using the disk diffusion method. Table 1 and (Supporting Information, Figure S1) showed the antimicrobial inhibition zone for undoped SO₂ and Ag-doped SnO₂ nanoparticles at concentrations ranging from 3 to 5.5 (mg/mL). Accordingly, for Undoped SO₂ nanoparticles,

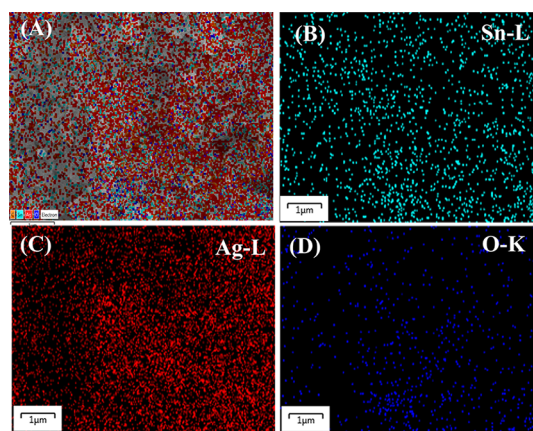


Figure 7. EDX mapping of Ag-doped SnO₂ NPs control (A), mapping area of Sn (B), mapping area of Ag (C), and mapping area of oxygen (D).

the highest concentration was found at 5 mg/mL, with the inhibition zones 11 ± 0.5 and 9.3 ± 0.35 mm for *S. aureus* and *E. coli* respectively. Similarly, for Ag-doped SnO₂ contents with 0.2Ag-doped SnO₂, 0.4Ag-doped SnO₂, 0.6Ag-doped SnO₂, 0.8Ag-doped SnO₂, and 1.0Ag-doped SnO₂, the corresponding inhibition zone at a concentration of 5 mg/mL was 18.3 ± 0.1 , 21 ± 1.09 , 24 ± 0.23 , 29 ± 0.54 , and 23.7 ± 0.45 mm for *S. aureus*, respectively, while for *E. coli* bacterial strain the corresponding inhibition zone was 17 ± 0.56 , 20 ± 0.80 , 23 ± 0.55 , 27 ± 0.05 , and 22.3 ± 0.63 mm, respectively. Among the Ag-doped SnO₂ contents, 0.8Ag-doped SnO₂ had the highest antibacterial activity with inhibition zones of 29 ± 0.54 and 27 ± 0.05 mm for *S. aureus* and *E. coli*, respectively, at a concentration of 5 mg/mL. From tested samples' results of

Table 1. Inhibition Zone (mm) of Pure SnO₂, and 0.2Ag-Doped SnO₂, 0.4Ag-Doped SnO₂, 0.6Ag-Doped SnO₂, 0.8Ag-Doped SnO₂, and Control Docymycine, Propiconazole, and Distilled Water^a

| samples | conc. (mg/mL) | microbial and inhibition zone (mm) | | | |
|------------------------|---------------|------------------------------------|----------------|---------------------|-----------------------|
| | | <i>S. aureus</i> | <i>E. coli</i> | <i>F. oxysporum</i> | <i>F. graminearum</i> |
| SnO ₂ | 3 | 9 ± 0.02 | 7 ± 0.94 | 4 ± 0.30 | 3 ± 0.13 |
| | 3.3 | 9 ± 0.15 | 7 ± 0.25 | 4 ± 0.03 | 3 ± 0.61 |
| | 4 | 10 ± 0.5 | 7.5 ± 0.36 | 5.5 ± 0.29 | 3 ± 0.40 |
| | 4.5 | 10.5 ± 0.2 | 9 ± 0.69 | 60 ± 0.51 | 3 ± 0.20 |
| | 5 | 11 ± 0.5 | 9.3 ± 0.35 | 6 ± 0.13 | 4.5 ± 0.61 |
| | 5.5 | 10.5 ± 0.12 | 8.5 ± 0.17 | 7 ± 0.22 | 5 ± 0.24 |
| 0.2Ag:SnO ₂ | 3 | 12 ± 0.3 | 11 ± 0.26 | 5 ± 0.36 | 4 ± 0.46 |
| | 3.3 | 12.5 ± 0.4 | 11.5 ± 0.71 | 6.45 ± 0.15 | 5.5 ± 0.77 |
| | 4 | 16 ± 0.25 | 11 ± 0.38 | 7 ± 0.03 | 6 ± 0.26 |
| | 4.5 | 17.5 ± 0.45 | 16 ± 0.42 | 7 ± 0.28 | 6 ± 0.60 |
| | 5 | 18.3 ± 0.1 | 17 ± 0.56 | 7.5 ± 0.22 | 6 ± 0.75 |
| | 5.5 | 17 ± 0.51 | 16.5 ± 0.11 | 8 ± 0.07 | 7.5 ± 0.20 |
| 0.4Ag:snO ₂ | 3 | 17 ± 0.32 | 16 ± 0.43 | 7 ± 0.12 | 6.5 ± 0.75 |
| | 3.3 | 17.5 ± 0.35 | 17 ± 0.25 | 7 ± 0.30 | 6.5 ± 0.20 |
| | 4 | 19 ± 0.79 | 17 ± 0.33 | 7 ± 0.78 | 6 ± 0.38 |
| | 4.5 | 19 ± 1.10 | 19 ± 0.50 | 7 ± 0.30 | 7 ± 0.10 |
| | 5 | 21 ± 1.09 | 20 ± 0.80 | 8.5 ± 0.19 | 7 ± 0.44 |
| | 5.5 | 20 ± 0.52 | 19.5 ± 0.81 | 9 ± 0.52 | 8 ± 0.41 |
| 0.6Ag:SnO ₂ | 3 | 20 ± 1.12 | 18 ± 0.39 | 10 ± 0.14 | 8.5 ± 0.42 |
| | 3.3 | 20 ± 0.34 | 20 ± 0.65 | 9.5 ± 0.73 | 8 ± 0.05 |
| | 4 | 22.5 ± 0.90 | 21.5 ± 0.11 | 10.5 ± 0.5 | 9 ± 0.35 |
| | 4.5 | 23 ± 0.23 | 21 ± 0.21 | 11 ± 0.22 | 9 ± 0.26 |
| | 5 | 24 ± 0.23 | 23 ± 0.55 | 11 ± 0.55 | 9 ± 0.31 |
| | 5.5 | 23 ± 0.45 | 21.5 ± 0.45 | 12 ± 0.16 | 11 ± 0.52 |
| 0.8Ag:SnO ₂ | 3 | 26.5 ± 0.97 | 23 ± 0.01 | 11 ± 0.41 | 10 ± 0.26 |
| | 3.3 | 27 ± 0.80 | 24 ± 0.61 | 13 ± 0.29 | 11 ± 0.37 |
| | 4 | 27 ± 0.46 | 25.5 ± 0.22 | 13 ± 0.21 | 12 ± 0.21 |
| | 4.5 | 27.5 ± 0.56 | 26 ± 0.13 | 14 ± 0.04 | 12 ± 0.16 |
| | 5 | 29 ± 0.54 | 27 ± 0.05 | 14.5 ± 0.24 | 13 ± 0.12 |
| | 5.5 | 28 ± 0.71 | 26 ± 0.34 | 17 ± 0.05 | 15 ± 0.05 |
| 1.0Ag:SnO ₂ | 3 | 23 ± 0.71 | 19 ± 0.79 | 14 ± 0.17 | 11 ± 0.28 |
| | 3.3 | 23 ± 0.33 | 19 ± 0.11 | 11 ± 0.17 | 12.5 ± 0.85 |
| | 4 | 23 ± 0.30 | 21.5 ± 0.44 | 12 ± 0.10 | 13 ± 0.27 |
| | 4.5 | 22 ± 0.50 | 20 ± 0.23 | 12 ± 0.45 | 13 ± 0.68 |
| | 5 | 23.7 ± 0.45 | 22.3 ± 0.63 | 15 ± 0.34 | 13.5 ± 0.09 |
| | 5.5 | 22 ± 0.21 | 21 ± 0.24 | 16 ± 0.76 | 14 ± 0.50 |
| docymycine | - | 36 ± 0.01 | 35 ± 0.03 | - | - |
| propiconazole | - | - | - | 29 ± 0.02 | 29 ± 0.01 |
| deionized water | - | - | - | - | - |

^aNote: “-” sign indicates no inhibition zone.

zone inhibition are typically displayed in the following order: 0.8Ag-doped SnO₂ > 0.6Ag-doped > 0.4Ag-doped > 0.2Ag-doped > undoped SnO₂ NPs. Thus, Ag-doped SnO₂ nanoparticles appeared to be more toxic to Gram-negative bacteria than to Gram-positive bacteria. The differences between these two different types of bacteria can be explained by the distinct structures and chemical compositions of the cell surfaces. In contrast to Gram-positive bacteria, which lack an outer membrane covering the peptidoglycan layer, Gram-negative bacteria have a layer in their cell walls. Thus, the outer membrane of Gram-negative bacteria may easily be damaged by Ag-doped SnO₂ NPs.⁶⁷ Furthermore, the green synthetic method of silver-doped tin oxide was reasonable for the nanoparticles' enhancement of the antibacterial activity. The reason for the high antibacterial activity of green synthesized Silver-doped Tin oxide is that the ginger plant extract contains a stabilizing agent that prevents agglomeration, which in turn

reduces the particle size of the synthesized nanoparticles.⁶⁸ Moreover, Docymycine and propiconazole were used as standard controls to compare the antibacterial activity of Ag-doped SnO₂ Nps, and the detailed results are shown in Table 1. The antifungal activity of the undoped SnO₂ NPs and Ag-doped SnO₂ NPs against *F. oxysporum* and *F. graminearum* was also presented in Table 1 and (Figure S2 Supporting Information). The obtained result showed that the 0.8Ag doped SnO₂ exhibit highest antifungal activity among Ag-doped SnO₂ contents with inhibition zones of 17 ± 0.05 and 15 ± 0.05 mm for *F. oxysporum*, and *F. graminearum*, respectively.

The effect of Ag doping into SnO₂ on antimicrobial activities may enhance the surface area and reactivity of SnO₂ nanoparticles, leading to increased contact with microbial cells and improved antimicrobial efficiency. In addition, Ag doping facilitates the sustained release of silver ions,

prolonging the antimicrobial effects of SnO₂ nanoparticles and enabling continuous interaction with microbial cells.^{33,69} The possible mechanism of antimicrobial activity of green synthesized Ag-doped SnO₂ is presented in Figure 8.

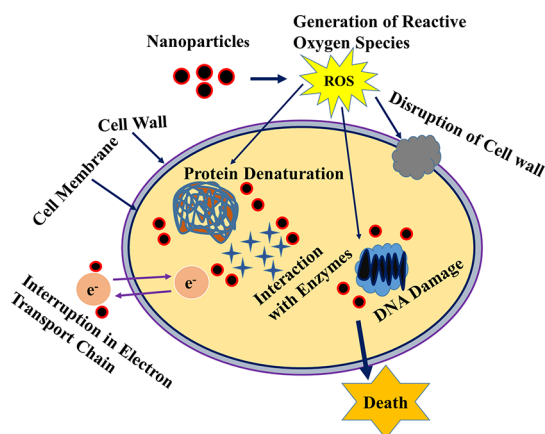


Figure 8. Possible schematic representation of the antimicrobial mechanism for Ag-doped SnO₂ nanoparticles.

Currently, the reported literature states that a number of mechanisms, including the production of reactive oxygen species (ROS), large small particle size or surface area of the nanoparticles, and efflux mechanisms leading to the release of constituent ions, have been proposed for the antimicrobial activity.⁷⁰

In this study, it is possible that the direct interaction of Ag-doped SnO₂ nanomaterials with the bacterial cell wall, followed by membrane penetration or disruption, may cause the membrane to become disorganized, inhibiting cell growth or ultimately resulting in cell death.⁶⁹ Furthermore, Ag can easily release Ag⁺ when it reacts with the cell membrane, then enters the cell, and may damage DNA, leading to mutation or death. In addition, according to reported literature, Ag-based nanoparticles have the ability to damage mitochondria in cells which causes a lack of energy and leads to cell death. Similarly, the destruction of the internal structure of cells caused by the interaction of Ag⁺ with the reactive oxygen species (ROS) generated by cells is another factor contributing to cell death.^{48,59,71} Generally, the antibacterial activity of Ag-doped SnO₂ nanoparticles likely involves a combination of ROS generation, cell membrane damage, release of silver ions, nanoparticle uptake, and potential synergistic effects, all contributing to the disruption and eventual death of bacterial cells.

Table 2 displays a comparison of the currently studied green synthesis of SnO₂ and Ag-doped SnO₂ nanoparticles with previously reported using chemical methods against *E. coli* and *S. aureus*. Thus, the inhibition zone of silver-doped tin oxide produced using the green synthesis approach is higher than that of all chemically produced silver-doped Tin oxide nanoparticles, this indicates that the green-generated silver-doped tin oxide exhibits higher antibacterial activity when compared to previously reported chemically synthesized silver-doped tin oxide.

4. CONCLUSIONS

In this study, an Ag-doped SnO₂ nanoparticle was synthesized by an ecofriendly green approach using mediated ginger (*Z.*

Table 2. Comparison of Antibacterial Activity of Green Synthesis Ag-Doped SnO₂ with Other Reported Literature Values

| nanoparticle | synthesis method | size (nm) | inhibition zone (mm) | | ref |
|---------------------------|--------------------|-----------|----------------------|----------------|------------------|
| | | | <i>S. aureus</i> | <i>E. coli</i> | |
| Ag-doped SnO ₂ | coprecipitation | 30 | 8 | 12 | ⁷² |
| Ag-doped SnO ₂ | electro spinning | 47 | 15 | 12 | ⁵⁹ |
| Ag-doped SnO ₂ | sol-gel | 35 | 18 | 19 | ⁵⁷ |
| SnO ₂ | sol-gel | 21 | 10 | 9 | ⁷³ |
| Ag-doped SnO ₂ | vapor phase growth | 29 | 17 | 18 | ⁷¹ |
| SnO ₂ | gel combustion | 41 | 9 | 8 | ^{74,75} |
| Ag-doped SnO ₂ | coprecipitation | 23 | 20 | 15 | ⁷⁶ |
| Ag-doped SnO ₂ | green method | 15 | 29 | 27 | this work |
| SnO ₂ | green method | 20 | 11 | 9 | |

officinale) root extract. The as-prepared samples were characterized by using UV-vis spectroscopy, X-ray diffraction (XRD), Fourier transforms infrared spectroscopy (FTIR), and scanning electron microscopy (SEM), and their antimicrobial activity was examined. According to XRD analysis, the green synthesized undoped and Ag-doped SnO₂ nanoparticles showed a tetragonal structure with an average crystallite size of between 10 and 17 nm. The vibration bands at 505.69 cm⁻¹ are particularly attributed to the O-Sn-O bending and stretching vibration of Sn-O and the absorption peaks observed at 622.239 cm⁻¹ are assigned to the Ag-O-Sn bonding of the Ag-doped SnO₂ composite particles. From EDX mapping and elemental analysis, strong evidence was confirmed that the silver ions have been successfully incorporated into the SnO₂. The green-synthesized Ag-doped SnO₂ nanoparticles showed significant antimicrobial activity against Gram-positive (*S. aureus*) and Gram-negative (*E. coli*) bacteria and fungi (*F. oxysporum* and *F. graminearum*). Ag-doped SnO₂ Nps relatively exhibit higher antibacterial activity against *S. aureus* and *E. coli*, indicating that bacteria are more sensitive to nanoparticles than fungi. Gram-negative bacteria's impermeable cell wall makes them more immune to antibiotics than Gram-positive bacteria. Moreover, it was found that the direct interaction of Ag-doped SnO₂ nanomaterials with the bacterial cell wall, followed by membrane disruption, may cause the membrane to become disorganized, inhibiting cell growth or ultimately resulting in cell death. This is because Ag can easily release Ag⁺ when it reacts with the cell membrane and then enters the cell and may damage DNA, leading to death. Thus, the current green synthesized Ag-doped SnO₂ nanoparticles have good prospects for the use of antimicrobial agents and other biomedical applications.

■ ASSOCIATED CONTENT

Supporting Information

The Supporting Information is available free of charge at <https://pubs.acs.org/doi/10.1021/acsomega.3c07855>.

Test of qualitative phytochemical screening of Ginger (*Z. officinale*) and its confirmation test result, image of Inhibition zone of bacteria for *S. aureus* and *E. coli*, and image of inhibition zone of fungi for *F. oxysporum* (A) and *F. graminearum* (B) (PDF)

AUTHOR INFORMATION

Corresponding Author

Tolesa Fita Chala – Department of Chemistry, College of Natural and Computational Science, Mattu University, Mattu 318, Ethiopia; orcid.org/0000-0002-8958-1969; Phone: +251913368922; Email: tolesafita@gmail.com

Authors

Yobsan Likasa Tiki – College of Natural and Computational Science, Department of Chemistry, Ambo University, Ambo 19, Ethiopia

Leta Deressa Tolesa – College of Applied Natural Science, Department of Applied Chemistry, Adama Science and Technology University, Adama 1888, Ethiopia

Ardila Hayu Tiwikrama – Department of Chemical Engineering and Biotechnology, National Taipei University of Technology, Taipei 106-344, Taiwan; orcid.org/0000-0002-0393-6774

Complete contact information is available at:

<https://pubs.acs.org/10.1021/acsomega.3c07855>

Author Contributions

Y.L.T.: Investigate the experiments, analyzed the result and wrote the manuscript. L.D.T.: Reviewed and revised the manuscript. A.H.T.: Characterize the samples using SEM. T.F.C.: Supervised the experiment, reviewed and revised the manuscript.

Notes

The authors declare no competing financial interest.

ACKNOWLEDGMENTS

The authors are highly grateful for financial support from Mattu University, Mattu, Oromia, Ethiopia

REFERENCES

- (1) Kolář, M.; Urbanek, K.; Látal, T. Antibiotic selective pressure and development of bacterial resistance. *International journal of antimicrobial agents* **2001**, *17* (5), 357–363.
- (2) Vega-Jiménez, A. L.; Vázquez-Olmos, A. R.; Acosta-Gío, E.; Álvarez-Pérez, M. A. In vitro antimicrobial activity evaluation of metal oxide nanoparticles. *Nanoemulsions Prop. Fabr. Appl.* **2019**, 1–18.
- (3) Gold, K.; Slay, B.; Knackstedt, M.; Gaharwar, A. K. Antimicrobial activity of metal and metal-oxide based nanoparticles. *Adv. Ther.* **2018**, *1* (3), No. 1700033.
- (4) Slavin, Y. N.; Asnis, J.; Háfeli, U. O.; Bach, H. Metal nanoparticles: understanding the mechanisms behind antibacterial activity. *J. Nanobiotechnol.* **2017**, *15*, 65.
- (5) Akbari, B.; Tavandashti, M. P.; Zandrahimi, M. Particle size characterization of nanoparticles—a practical approach. *Iran. J. Mater. Sci. Eng.* **2011**, *8* (2), 48–56.
- (6) Li, Y.; Xia, Y.; Liu, K.; Ye, K.; Wang, Q.; Zhang, S.; Huang, Y.; Liu, H. Constructing Fe-MOF-derived Z-scheme photocatalysts with enhanced charge transport: nanointerface and carbon sheath synergistic effect. *ACS Appl. Mater. Interfaces* **2020**, *12* (22), 25494–25502.
- (7) Bukhari, A.; Ijaz, I.; Gilani, E.; Nazir, A.; Zain, H.; Saeed, R.; Alarfaji, S. S.; Hussain, S.; Aftab, R.; Naseer, Y. Green synthesis of metal and metal oxide nanoparticles using different plants' parts for antimicrobial activity and anticancer activity: a review article. *Coatings* **2021**, *11* (11), 1374.
- (8) Sagadevan, S.; Lett, J. A.; Fatimah, I.; Lokanathan, Y.; Léonard, E.; Oh, W. C.; Hossain, M. M.; Johan, M. R. Current trends in the green syntheses of tin oxide nanoparticles and their biomedical applications. *Materials Research Express* **2021**, *8* (8), No. 082001.
- (9) Soltys, L.; Olkhovyy, O.; Tatarchuk, T.; Naushad, M. Green synthesis of metal and metal oxide nanoparticles: Principles of green chemistry and raw materials. *Magnetochemistry* **2021**, *7* (11), 145.
- (10) Das, R. K.; Pachapur, V. L.; Lonappan, L.; Naghdi, M.; Pulicharla, R.; Maiti, S.; Cledon, M.; Dalila, L. M. A.; Sarma, S. J.; Brar, S. K. Biological synthesis of metallic nanoparticles: plants, animals and microbial aspects. *Nanotechnol. Environ. Eng.* **2017**, *2*, 18.
- (11) Patra, S.; Mukherjee, S.; Barui, A. K.; Ganguly, A.; Sreedhar, B.; Patra, C. R. Green synthesis, characterization of gold and silver nanoparticles and their potential application for cancer therapeutics. *Materials Science and Engineering: C* **2015**, *53*, 298–309.
- (12) Jeevanandam, J.; Chan, Y. S.; Danquah, M. K. Biosynthesis of metal and metal oxide nanoparticles. *ChemBioEng. Reviews* **2016**, *3* (2), 55–67.
- (13) Babu, A. T.; Antony, R. Green synthesis of silver doped nano metal oxides of zinc & copper for antibacterial properties, adsorption, catalytic hydrogenation & photodegradation of aromatics. *Journal of Environmental Chemical Engineering* **2019**, *7* (1), No. 102840.
- (14) Narasaiah, B. P.; Banoth, P.; Sohan, A.; Mandal, B. K.; Bustamante Dominguez, A. G.; De Los Santos Valladares, L.; Kollu, P. Green biosynthesis of tin oxide nanomaterials mediated by agro-waste cotton boll peel extracts for the remediation of environmental pollutant dyes. *ACS omega* **2022**, *7* (18), 15423–15438.
- (15) Fouda, A.; Eid, A. M.; Guibal, E.; Hamza, M. F.; Hassan, S. E.-D.; Alkhalifah, D. H. M.; El-Hossary, D. Green Synthesis of Gold Nanoparticles by Aqueous Extract of Zingiber officinale: Characterization and Insight into Antimicrobial, Antioxidant, and In Vitro Cytotoxic Activities. *Applied Sciences* **2022**, *12* (24), 12879.
- (16) Menon, S.; KS, S. D.; Agarwal, H.; Shanmugam, V. K. Efficacy of biogenic selenium nanoparticles from an extract of ginger towards evaluation on anti-microbial and anti-oxidant activities. *Colloid Interface Sci. Commun.* **2019**, *29*, 1–8.
- (17) Abbas, A. H.; Fairouz, N. Y. Characterization, biosynthesis of copper nanoparticles using ginger roots extract and investigation of its antibacterial activity. *Materials Today: Proceedings* **2022**, *61*, 908–913.
- (18) Saeed, Z.; Pervaiz, M.; Ejaz, A.; Hussain, S.; Shaheen, S.; Shehzad, B.; Younas, U. Garlic and ginger extracts mediated green synthesis of silver and gold nanoparticles: A review on recent advancements and prospective applications'. *Biocatalysis and Agricultural Biotechnology* **2023**, *53*, No. 102868.
- (19) Velmurugan, P.; Anbalagan, K.; Manosathyadevan, M.; Lee, K.-J.; Cho, M.; Lee, S.-M.; Park, J.-H.; Oh, S.-G.; Bang, K.-S.; Oh, B.-T. Green synthesis of silver and gold nanoparticles using Zingiber officinale root extract and antibacterial activity of silver nanoparticles against food pathogens. *Bioprocess Biosyst. Eng.* **2014**, *37*, 1935–1943.
- (20) Abdullah; Hussain, T.; Faisal, S.; Rizwan, M.; Almostafa, M. M.; Younis, N. S.; Yahya, G. Zingiber officinale rhizome extracts mediated ni nanoparticles and its promising biomedical and environmental applications. *BMC Complement. Med. Ther.* **2023**, *23* (1), 349.
- (21) Salwa, A.; Ahmed, A. E.-S.; Wasly, H.; Abd El-Sadek, M. SnO2 Nanoparticles: Green Synthesis, Characterization, and Water Treatment. *ECS Journal of Solid State Science and Technology* **2022**, *11* (10), 103005.
- (22) Elango, G.; Kumaran, S. M.; Kumar, S. S.; Muthuraja, S.; Roopan, S. M. Green synthesis of SnO2 nanoparticles and its photocatalytic activity of phenolsulfonphthalein dye. *Spectrochimica Acta Part A: Molecular and Biomolecular Spectroscopy* **2015**, *145*, 176–180.
- (23) Selvakumari, J. C.; Ahila, M.; Malligavathy, M.; Padiyan, D. P. Structural, morphological, and optical properties of tin (IV) oxide nanoparticles synthesized using Camellia sinensis extract: a green approach. *International Journal of Minerals, Metallurgy, and Materials* **2017**, *24*, 1043–1051.
- (24) Dheyab, M. A.; Aziz, A. A.; Jameel, M. S.; Oladzadabbasabadi, N. Recent advances in synthesis, modification, and potential application of tin oxide nanoparticles. *Surfaces and Interfaces* **2022**, *28*, No. 101677.
- (25) Uday, Y.; Manjunatha, H.; Vidya, Y.; Manjunatha, S.; Soundar, R.; Sridhar, K. Multifunctional properties of tin oxide nanoparticles

- synthesized by green and chemical approach. *Curr. Appl. Phys.* **2023**, *55*, 9–15.
- (26) Rebecca, B. N.; Verena, C.; Gerhard, F.; Karl, F. Indium and Indium Tin Oxide Induce Endoplasmic Reticulum Stress and Oxidative Stress in Zebrafish (*Danio rerio*). *Environ. Sci. Technol.* **2014**, *48*, 11679–11687, DOI: 10.1021/es5034876.
- (27) Qamar, M.; Shahid, S.; Khan, S.; Zaman, S.; Sarwar, M. Synthesis characterization, optical and antibacterial studies of Co-doped SnO₂ nanoparticles. *Dig. J. Nanomater. Biostruct.* **2017**, *12* (4), 1127–1135.
- (28) Amutha, T.; Rameshbabu, M.; Sasi Florence, S.; Senthilkumar, N.; Vetha Potheher, I.; Prabha, K. Studies on structural and optical properties of pure and transition metals (Ni, Fe and co-doped Ni-Fe) doped tin oxide (SnO₂) nanoparticles for anti-microbial activity. *Res. Chem. Intermed.* **2019**, *45*, 1929–1941.
- (29) Haq, S.; Rehman, W.; Waseem, M.; Shah, A.; Khan, A. R.; Rehman, M. U.; Ahmad, P.; Khan, B.; Ali, G. Green synthesis and characterization of tin dioxide nanoparticles for photocatalytic and antimicrobial studies. *Materials Research Express* **2020**, *7* (2), No. 025012.
- (30) Fatimah, I. Green synthesis of silver nanoparticles using extract of *Parkia speciosa* Hassk pods assisted by microwave irradiation. *Journal of advanced research* **2016**, *7* (6), 961–969.
- (31) Kang, J.; Jin, W.; Wang, J.; Sun, Y.; Wu, X.; Liu, L. Antibacterial and anti-biofilm activities of peppermint essential oil against *Staphylococcus aureus*. *Lwt* **2019**, *101*, 639–645.
- (32) Parthibavarman, M.; Sathishkumar, S.; Jayashree, M.; BoopathiRaja, R. Microwave assisted synthesis of pure and Ag doped SnO₂ quantum dots as novel platform for high photocatalytic activity performance. *Journal of Cluster Science* **2019**, *30* (2), 351–363.
- (33) Mahjouri, S.; Kosari-Nasab, M.; Kazemi, E. M.; Divband, B.; Movafeghi, A. Effect of Ag-doping on cytotoxicity of SnO₂ nanoparticles in tobacco cell cultures. *J. Hazard. Mater.* **2020**, *381*, No. 121012.
- (34) Xinping, L.; Shengli, L.; Miaotao, Z.; Wenlong, Z.; Chuanghong, L. Evaluations of antibacterial activity and cytotoxicity on Ag nanoparticles. *Rare Metal Materials and Engineering* **2011**, *40* (2), 209–214.
- (35) Guo, L.; Liang, H.; An, D.; Yang, H. One-step hydrothermal synthesis of uniform Ag-doped SnO₂ nanoparticles for highly sensitive ethanol sensing. *Physica E: Low-dimensional Systems and Nanostructures* **2023**, *151*, No. 115717.
- (36) Saravanakumar, K.; Muthuraj, V. Fabrication of sphere like plasmonic Ag/SnO₂ photocatalyst for the degradation of phenol. *Optik* **2017**, *131*, 754–763.
- (37) Khojasteh, F.; Mersagh, M. R.; Hashemipour, H. The influences of Ni, Ag-doped TiO₂ and SnO₂, Ag-doped SnO₂/TiO₂ nanocomposites on recombination reduction in dye synthesized solar cells. *J. Alloys Compd.* **2022**, *890*, No. 161709.
- (38) Lu, Z.; Zhou, Q.; Xu, L.; Gui, Y.; Zhao, Z.; Tang, C.; Chen, W. Synthesis and characterization of highly sensitive hydrogen (H₂) sensing device based on Ag doped SnO₂ nanospheres. *Materials* **2018**, *11* (4), 492.
- (39) Kolhe, P. S.; Koinkar, P. M.; Maiti, N.; Sonawane, K. M. Synthesis of Ag doped SnO₂ thin films for the evaluation of H₂S gas sensing properties. *Physica B: Condensed Matter* **2017**, *524*, 90–96.
- (40) Huang, Y.; Guo, Z.; Liu, H.; Zhang, S.; Wang, P.; Lu, J.; Tong, Y. Heterojunction architecture of N-doped WO₃ nanobundles with Ce₂S₃ nanodots hybridized on a carbon textile enables a highly efficient flexible photocatalyst. *Adv. Funct. Mater.* **2019**, *29* (45), 1903490.
- (41) Korotcenkov, G.; Boris, I.; Brinzari, V.; Han, S.; Cho, B. The role of doping effect on the response of SnO₂-based thin film gas sensors: Analysis based on the results obtained for Co-doped SnO₂ films deposited by spray pyrolysis. *Sens. Actuators, B* **2013**, *182*, 112–124.
- (42) Gu, C.; Guan, W.; Liu, X.; Gao, L.; Wang, L.; Shim, J.-J.; Huang, J. Controlled synthesis of porous Ni-doped SnO₂ microstructures and their enhanced gas sensing properties. *J. Alloys Compd.* **2017**, *692*, 855–864.
- (43) Khan, S. A.; Kanwal, S.; Rizwan, K.; Shahid, S. Enhanced antimicrobial, antioxidant, in vivo antitumor and in vitro anticancer effects against breast cancer cell line by green synthesized un-doped SnO₂ and Co-doped SnO₂ nanoparticles from *Clerodendrum inerme*. *Microbial pathogenesis* **2018**, *125*, 366–384.
- (44) Haider, A.; Ijaz, M.; Ali, S.; Haider, J.; Imran, M.; Majeed, H.; Shahzadi, I.; Ali, M. M.; Khan, J. A.; Ikram, M. Green synthesized phytochemically (*Zingiber officinale* and *Allium sativum*) reduced nickel oxide nanoparticles confirmed bactericidal and catalytic potential. *Nanoscale Res. Lett.* **2020**, *15*, 1–11.
- (45) Ahmed, S.; Ahmad, M.; Swami, B. L.; Ikram, S. A review on plants extract mediated synthesis of silver nanoparticles for antimicrobial applications: a green expertise. *Journal of advanced research* **2016**, *7* (1), 17–28.
- (46) Karthik, K.; Revathi, V.; Tatarchuk, T. Microwave-assisted green synthesis of SnO₂ nanoparticles and their optical and photocatalytic properties. *Mol. Cryst. Liq. Cryst.* **2018**, *671* (1), 17–23.
- (47) Ersöz, E.; Altintas Yildirim, O. Green synthesis and characterization of Ag-doped ZnO nanofibers for photodegradation of MB, RhB and MO dye molecules. *Journal of the Korean Ceramic Society* **2022**, *59* (5), 655–670.
- (48) Sunny, N. E.; Shanmugam, V. K. Anti-blight effect of green synthesized pure and Ag-doped tin oxide nanoparticles from *Averrhoa bilimbi* fruit extract towards *Xanthomonas oryzae*-the leaf blight pathogen of rice. *Inorg. Chem. Commun.* **2021**, *133*, No. 108866.
- (49) Arawande, J. O.; Akinnusotu, A.; Alademeyin, J. O. Extractive value and phytochemical screening of ginger (*Zingiber officinale*) and turmeric (*Curcuma longa*) using different solvents. *Int. J. Trad. Nat. Med.* **2018**, *8* (1), 13–22.
- (50) Varadharajan, V.; Janarthanan, U. K.; Krishnamurthy, V. Physicochemical, phytochemical screening and profiling of secondary metabolites of *Annona squamosa* leaf extract. *World J. Pharm. Res.* **2012**, *1* (4), 1143–1164.
- (51) Mehata, M. S. Green route synthesis of silver nanoparticles using plants/ginger extracts with enhanced surface plasmon resonance and degradation of textile dye. *Materials Science and Engineering: B* **2021**, *273*, No. 115418.
- (52) Yadi, M.; Azizi, M.; Dianat-Moghadam, H.; Akbarzadeh, A.; Abyadeh, M.; Milani, M. Antibacterial activity of green gold and silver nanoparticles using ginger root extract. *Bioprocess Biosyst. Eng.* **2022**, *45* (12), 1905–1917.
- (53) Sahu, M.; Biswas, P. Single-step processing of copper-doped titania nanomaterials in a flame aerosol reactor. *Nanoscale Res. Lett.* **2011**, *6*, 441.
- (54) Choudhury, B.; Dey, M.; Choudhury, A. Defect generation, d-d transition, and band gap reduction in Cu-doped TiO₂ nanoparticles. *Int. Nano Lett.* **2013**, *3*, 1–8.
- (55) Liu, D.; Pan, J.; Tang, J.; Liu, W.; Bai, S.; Luo, R. Ag decorated SnO₂ nanoparticles to enhance formaldehyde sensing properties. *J. Phys. Chem. Solids* **2019**, *124*, 36–43.
- (56) Garrafa-Galvez, H.; Nava, O.; Soto-Robles, C.; Vilchis-Nestor, A.; Castro-Beltrán, A.; Luque, P. Green synthesis of SnO₂ nanoparticle using *Lycopersicon esculentum* peel extract. *J. Mol. Struct.* **2019**, *1197*, 354–360.
- (57) Nair, K. K.; Kumar, P.; Kumar, V.; Harris, R.; Kroon, R.; Viljoen, B.; Shumbula, P.; Mlambo, M.; Swart, H. Synthesis and evaluation of optical and antimicrobial properties of Ag-SnO₂ nanocomposites. *Phys. B: Condens. Matter* **2018**, *535*, 338–343.
- (58) Shuvo, M. S. H.; Putul, R. A.; Hossain, K. S.; Masum, S. M.; Molla, M. A. I. Photocatalytic Removal of Metronidazole Antibiotics from Water Using Novel Ag-N-SnO₂ Nanohybrid Material. *Toxics* **2024**, *12* (1), 36.
- (59) Li, Y.; Gao, S.; Zhang, B.; Mao, H.; Tang, X. Electrospun Ag-doped SnO₂ hollow nanofibers with high antibacterial activity. *Electronic Materials Letters* **2020**, *16*, 195–206.

(60) Anusha, G.; Noori, M. T.; Ghangrekar, M. Application of silver-tin dioxide composite cathode catalyst for enhancing performance of microbial desalination cell. *Materials Science for Energy Technologies* **2018**, *1* (2), 188–195.

(61) Hu, M.; Zhang, Z.; Luo, C.; Qiao, X. One-pot green synthesis of Ag-decorated SnO₂ microspheres: an efficient and reusable catalyst for reduction of 4-nitrophenol. *Nanoscale Res. Lett.* **2017**, *12*, 435.

(62) Mützel, T.; Hubrich, C. Effect of Additives on the Switching Performance of Ag/SnO₂ under AC-3 Conditions; In *2019 IEEE Holm Conference on Electrical Contacts*; IEEE, 2019, pp. 1–7.

(63) Franco, V.; Béron, F.; Pirota, K.; Knobel, M.; Willard, M. Characterization of the magnetic interactions of multiphase magneto-caloric materials using first-order reversal curve analysis. *J. Appl. Phys.* **2015**, *117*, 17.

(64) Shittu, H. A.; Adedokun, O.; Kareem, M. A.; Sivaprakash, P.; Bello, I. T.; Arumugam, S. Effect of low-doping concentration on silver-doped SnO₂ and its photocatalytic applications. *Biointerface Res. Appl. Chem.* **2023**, *13*, 165.

(65) Nasir, Z.; Shakir, M.; Wahab, R.; Shoeb, M.; Alam, P.; Khan, R. H.; Mobin, M. Co-precipitation synthesis and characterization of Co doped SnO₂ NPs, HSA interaction via various spectroscopic techniques and their antimicrobial and photocatalytic activities. *Int. J. Biol. Macromol.* **2017**, *94*, 554–565.

(66) Habte, A. G.; Hone, F. G.; Dejene, F. B. Zn doping effect on the properties of SnO₂ nanostructure by co-precipitation technique. *Appl. Phys. A: Mater. Sci. Process.* **2019**, *125*, 402.

(67) Khalid, A.; Ahmad, P.; Alharthi, A. I.; Muhammad, S.; Khandaker, M. U.; Faruque, M. R. I.; Din, I. U.; Alotaibi, M. A.; Khan, A. Synergistic effects of Cu-doped ZnO nanoantibiotic against Gram-positive bacterial strains. *PLoS One* **2021**, *16* (5), No. e0251082.

(68) Sharma, N.; Kumar, J.; Thakur, S.; Sharma, S.; Shrivastava, V. Antibacterial study of silver doped zinc oxide nanoparticles against *Staphylococcus aureus* and *Bacillus subtilis*. *Drug Invention Today* **2013**, *5* (1), 50–54.

(69) Kumar, V.; Prakash, J.; Singh, J. P.; Chae, K. H.; Swart, C.; Ntwaeaborwa, O.; Swart, H.; Dutta, V. Role of silver doping on the defects related photoluminescence and antibacterial behaviour of zinc oxide nanoparticles. *Colloids Surf, B* **2017**, *159*, 191–199.

(70) Chandran, D.; Nair, L. S.; Balachandran, S.; Rajendra Babu, K.; Deepa, M. Structural, optical, photocatalytic, and antimicrobial activities of cobalt-doped tin oxide nanoparticles. *J. Sol-Gel Sci. Technol.* **2015**, *76*, 582–591.

(71) Tibayan, E. B., Jr; Muflikhun, M. A.; Kumar, V.; Fisher, C.; Al Rey, C. V.; Santos, G. N. C. Performance evaluation of Ag/SnO₂ nanocomposite materials as coating material with high capability on antibacterial activity. *Ain Shams Eng. J.* **2020**, *11* (3), 767–776.

(72) John, N.; Somaraj, M.; Tharayil, N. J. Synthesis, Characterization and Anti-bacterial Activities of Pure and Ag-doped SnO₂ Nanoparticles. *Materials Today: Proceedings* **2017**, *4* (2), 4351–4357.

(73) Khanom, R.; Parveen, S.; Hasan, M. Antimicrobial activity of SnO₂ nanoparticles against *Escherichia coli* and *Staphylococcus aureus* and conventional antibiotics. *Am. Sci. Res. J. Eng. Technol. Sci.* **2018**, *46* (1), 111–121.

(74) Bhosale, M. S.; Sarvanan, K.; Dighe, N. Recent Progress on Synthesis and Bio-activities of Tetrahydropyrimidine-2-one derivatives. *Research Journal of Science and Technology* **2021**, *13* (3), 221–228.

(75) Jalali, S. A. H.; Allafchian, A. R. Assessment of antibacterial properties of novel silver nanocomposite. *Journal of the Taiwan Institute of Chemical Engineers* **2016**, *59*, 506–513.

(76) Gurunathan, S.; Han, J. W.; Kwon, D.-N.; Kim, J.-H. Enhanced antibacterial and anti-biofilm activities of silver nanoparticles against Gram-negative and Gram-positive bacteria. *Nanoscale Res. Lett.* **2014**, *9*, 373 DOI: 10.1186/1556-276X-9-373.